Soils and Rocks
An International Journal of Geotechnical and Geoenvironmental Engineering
www.soilsandrocks.com
ISSN 1980-9743
ISSN-e 2675-5475

Understanding fine soil deformation in pavements: a master curve-based investigation for Amazon soils

Bruno Cavalcante Mota[1], Mariluce de Oliveira Ubaldo[1],
Daniela Muniz D'Antona Guimarães[2], Caroline Dias Amancio de Lima[3],
Lilian Ribeiro de Rezende[4], Luis Alberto Herrmann do Nascimento[5],
Francisco Thiago Sacramento Aragão[1#]

Article

Keywords:
Tropical soils
Master curves
Resilient modulus
Permanent deformation
Repeated load triaxial tests

Abstract

The performance of soils and granular materials must be considered in relation to the main deterioration mechanisms in pavement structure design. This study aims to evaluate the use of fine-grained soils as unbound materials in pavement applications. For this purpose, physical, chemical, and mechanical characterization tests were conducted. Repeated load triaxial tests were performed following current Brazilian standards and considering different soil saturation conditions. Five widely used mathematical models were employed to assess the resilient modulus under different moisture conditions, with the Compound and Universal models showing the best correlations. As moisture content increased, a reduction in resilient modulus was observed at higher stress levels. Regarding permanent deformation, the master curve approach was applied to obtain the parameters adopted as inputs for simulations within the mechanistic-empirical pavement design software, FlexPaveBR version 2.1.5. The model results adequately represented the plastic behavior of the analyzed conditions. The simulation results indicated differences between considering bonded and unbonded granular layers. The results also indicated that the use of fine-grained soils without stabilization can be considered for subbase layers, provided that triaxial testing is conducted and the materials demonstrate satisfactory performance under mechanistic-empirical evaluation.

1. Introduction

Pavements are multi-layered structures designed to improve driving conditions, comfort, economy, and safety (Bernucci et al., 2022). They are classified as rigid, semi-rigid, or flexible, with flexible pavements exhibiting elastic deformation across all layers, ensuring even stress distribution (DNIT, 2006). The base and subbase layers support the upper layers, while subgrade reinforcement may be required based on its strength. Huang (2004) found that granular layers contribute with 68% of total permanent deformation, emphasizing the need to study their effects.

Soil classification in geotechnical engineering considers factors such as origin, evolution, structure, and mechanical behavior. Classifications based on particle type and behavior are widely used due to their practical applications in soil identification and performance prediction. Brazil's diverse pedological spectrum includes Argisols, Latosols, and Chernozems, among others. Due to tropical climate conditions, traditional classification systems such as those from the American Association of State Highway and Transportation Officials (AASHTO) and the Unified Soil Classification System (USCS) are ineffective in accurately predicting mechanical behavior.

The capital of Amazonas, Manaus, presents distinctive geological characteristics due to its location at the center of the Amazon Sedimentary Basin, predominantly within the Alter do Chão Formation. This formation is mainly composed of sandstones, such as the Manaus Sandstone, along with siltstones and mudstones. It is overlain by a thick clay layer, which leads to a scarcity of surface rock material deposits - a common condition throughout much of the Amazon region (Falesi, 1972; Lima et al., 2006).

#Corresponding author. E-mail address: fthiago@coc.ufrj.br
[1]Universidade Federal do Rio de Janeiro, Programa de Pós-graduação em Engenharia Civil, Rio de Janeiro, RJ, Brasil.
[2]Universidade Federal do Amazonas, Departamento de Engenharia Civil, Manaus, AM, Brasil.
[3]Universidade Federal da Bahia, Programa de Pós-graduação em Engenharia Civil, Salvador, BA, Brasil.
[4]Universidade Federal de Goiás, Programa de Pós-graduação em Geotecnia, Estruturas e Construção Civil, Goiânia, GO, Brasil.
[5]Petrobras, Centro de Pesquisas Leopoldo Américo Miguez de Mello, Rio de Janeiro, RJ, Brasil.

Submitted on July 18, 2025; Final Acceptance on February 26, 2026; Discussion open until November 30, 2026.
Editor: Renato P. Cunha
https://doi.org/10.28927/SR.2026.011125

To address the unique behavior of tropical soils in pavement applications, the MCT classification was developed to categorize them into seven groups, distinguishing between lateritic and non-lateritic materials. This method, proposed by Nogami et al. (1989) and Nogami and Villibor (1991), is based on small-scale testing, limited to soils passing through a 2.00 mm sieve, and has been widely applied in transportation infrastructure studies.

Beyond classification, Permanent Deformation (*PD*) and Resilient Modulus (*RM*) tests are fundamental for pavement structural analyses. The *PD* test measures non-recoverable deformation, while the *RM* test evaluates recoverable deformation. These parameters are incorporated into mechanistic-empirical pavement design software, such as FlexPaveBR, improving structural analysis and optimization.

In 2018, Coppe initiated a Cooperation Agreement with Petrobras, UFRGS, and NCSU aimed at updating the Brazilian pavement design method and conducting a multiscale experimental investigation of asphalt mixtures and materials. As part of this initiative, the Guimarães (2009) model was integrated into FlexPave, a mechanistic-empirical pavement design software developed at NCSU. This integration resulted in a Brazilian version of the software, named FlexPaveBR, which incorporates national design practices and local material behavior. FlexPaveBR is available to the institutions involved in its validation (Coppe/UFRJ, Cenpes/Petrobras, and UFRGS), ensuring its application is aligned with Brazilian design practices.

However, the *PD* test, as standardized by DNIT 179 (2018b), is time-consuming, requiring six to nine stress pairs with 150,000 load cycles per pair, taking six to nine business days per sample. Several national and international studies have analyzed *PD* behavior in soils and granular materials (Monismith et al., 1975; Dawson and Wellner, 1999; Werkmeister et al., 2001; Kim et al., 2004; Tutumluer and Pan, 2008; Cerni et al., 2012; Lima et al., 2019; Pascoal et al., 2023; Sagrilo et al., 2023; Lima et al., 2023). Research has also explored ways to reduce the number of load cycles, apply multi-stage testing, and improve plastic behavior modeling (Silva et al., 2021; Lima et al., 2021; Cabral et al., 2021; Araújo et al., 2024; Mota et al., 2024).

Recognizing the need to optimize *PD* testing, Mota et al. (2024) proposed a master curve-based method, reducing load cycles per stress pair from 150,000 to 10,000, except for the most severe pair (120/360 kPa). Given this context, this study aims to analyze the physical, chemical, and mechanical properties of fine soils like those found in Manaus, Amazonas, providing a framework for their application in pavement layers. The findings contribute to optimizing the use of available natural resources and preventing the exclusion of potentially viable materials due to the limitations of other classification systems, particularly considering the Amazon region, where suitable aggregate sources are scarce.

2. Fine soils of the metropolitan region of Manaus, AM

The geodiversity of the Amazon, particularly influenced by the Alter do Chão and Solimões formations, results in a wide variety of soils whose properties are directly affected by intense weathering processes. In some areas, soft soils or highly plastic clays predominate, which are unsuitable for engineering applications due to their low strength and high deformability. However, in other regions, weathering has led to the formation of lateritic profiles, where more resistant soils, such as piçarra, are found. These materials are suitable for paving and other infrastructure applications. This variability in soil types demands site-specific geotechnical solutions, making detailed analysis essential to ensure both the technical and economic feasibility of construction projects in the region (Falesi, 1972).

The soils analyzed in this study were used as embankment (Soil 1) and subbase (Soil 2) layers in a roadway and as a subbase layer in an airport (Soil 3). The compaction energies were selected based on the intended use of these materials as reinforcement and sub-base layers in pavement structures. Figure 1 presents the specific locations of the materials.

The soils were collected from the B horizon using disturbed samples. In the laboratory, they underwent physical characterization through particle size distribution and Atterberg limits tests, following Brazilian standards (ABNT, 2016a; ABNT, 2016b; ABNT, 2016c). Table 1 presents the average physical and chemical properties and soil classifications. In terms of particle size, 66% of Soil 1 particles were smaller than 0.002 mm, classifying it as clay, while Soil 2 contains 26% clay and Soil 3, 38%.

The MCT classification (DNIT, 2023a, 2023b, 2023c) identified Soil 1 as non-lateritic clayey (NG'), exhibiting high load-bearing capacity, low to intermediate permeability, and moderate to high expansion, which may limit its use in higher-quality pavement layers such as the base. Soil 2 was classified as lateritic sandy (LA'), with high load-bearing capacity and lower moisture-induced expansion and contraction. Soil 3, in turn, was classified as lateritic clayey (LG'), with high load-bearing capacity, low expansion, and low permeability, making it suitable for pavement subgrade layers.

According to the AASHTO classification, the soils correspond to A-7-5, A-2-6, and A-6, respectively. The comparison between MCT, AASHTO, and USCS classifications highlights the need for methodologies adapted to tropical soils. Based on conventional systems, these materials would likely be considered unsuitable for pavement structures, reinforcing the importance of specialized evaluations.

In addition to physical and particle size analyses, energy-dispersive X-ray fluorescence (EDXRF) tests were conducted to determine elemental composition. The spectral peaks corresponded to different chemical elements, with higher peaks indicating greater concentrations. The results revealed iron (Fe), aluminum (Al), and titanium (Ti) - elements commonly found in lateritic soils of tropical regions such as Manaus.

Figure 1. Soil sampling locations in the metropolitan region of Manaus (Amazonas), Brazil.

Table 1. Physical and chemical characterization of soils in the metropolitan region of Manaus.

Physical characterization				Chemical analysis, Classifications, and Compaction tests			
	Soil 1	**Soil 2**	**Soil 3**		**Soil 1**	**Soil 2**	**Soil 3**
Liquid Limit (w_L) %	66	38	34	MCT - Brazilian Classification	NG'	LA'	LG'
Plastic Limit (w_P) %	40	25	23	AASHTO Classification	A-7-5	A-2-6	A-6
Plasticity Index (*PI*) %	26	13	11	Energy / Condition	Intermediate Energy (IE)	Modified Energy (ME)	Intermediate Energy (IE)
Specific Weight (γ) kN/m³	25.4	22.8	25.0	*OMC* (%)	33.0	10.7	17.0
% coarse sand (0.6-2.0mm)	2.2	24.8	11.6	*MDD* (kg/m³)	1370	2030	1782
% medium sand (0.2-0.6mm)	7.9	32.5	28.4	Most frequent chemical components	SiO_2, Al_2O_3, Fe_2O_3	SiO_2, Al_2O_3	SiO_2, Al_2O_3, Fe_2O_3
% fine sand (0.06-0.2mm)	6.6	15.3	11.0	California Bearing Ratio (*CBR*) (%)	19	45	25
% silt (2µm-0.06mm)	15.1	0.2	8.4	Expansion (%)	0.04	0.02	0.04
% clay (%< 2µm)	65.9	26.0	38.1				

Note: Results of granulometry refer only to analysis with dispersant.

A detailed analysis of these findings and their correlation with soil deformation behavior is presented in the results section.

3. Methodology

3.1 Test parameters

The experimental program consisted of five stages: (1) collection of disturbed soil samples; (2) physical, chemical, and mechanical characterization; (3) repeated load triaxial tests for *RM* and *PD*, including five models for resilient behavior analysis and the application of the Guimarães (2009) model and master curves (Mota et al., 2024) to determine permanent deformation parameters; (4) shakedown analysis, based on Werkmeister et al. (2001); and (5) pavement structural analysis, using the studied materials in the subbase layer under two traffic levels, incorporating the FlexPaveBR software adapted to the *PD* model proposed by Guimarães (2009).

The repeated load triaxial test simulates deviatoric and confining stress configurations in laboratory conditions. Linear Variable Differential Transformer (*LVDT*) transducers were attached to lightweight aluminum clamps at the top of the specimen, enclosed in a rubber membrane (Medina and Motta, 2015).

To standardize testing procedures, Brazilian standards DNIT 179 (2018b) and DNIT 134 (2018a), were established, leading to technical adjustments. These standards define *PD* and *RM* evaluations, detailing triaxial test procedures. For *RM*, two *LVDT* transducers (4 mm capacity) were installed inside the triaxial chamber, supported on a top cap that receives deviatoric stress through a load cell and piston. For *PD*, due to the high clay content, two *LVDT* transducers (25 mm capacity) were used.

The samples were compacted using intermediate and modified energies (Table 1). The compaction energy for each soil reflected both field application and laboratory performance. Soil 2 performed poorly under lower energies, requiring modified energy to ensure adequate behavior. The validity criterion for sample molding was a maximum variation of ±0.5% relative to the optimum moisture content (*OMC*), as per DNIT 134 and DNIT 179 (DNIT, 2018a and DNIT, 2018b, respectively). Since these standards do not specify an acceptable variation for maximum dry density (*MDD*), a ±1.0% limit was adopted.

The stiffness of compacted soils was evaluated through *RM* testing, following DNIT 134 (2018a). After conditioning, 18 pairs of deviatoric and confining stresses were applied per standard specifications. Testing was conducted under a 1 Hz repeated load frequency, with a 0.1-second load pulse and 0.9 seconds of rest. Plastic deformation and permanent deformation parameters were determined based on DNIT 179 (2018b) guidelines for sample preparation and the optimized *PD* methodology using master curves (Mota et al., 2024), which recommend the number of loading cycles and the stress pairs to be applied in the tests.

3.2 Mathematical models for *RM*

The *RM* test assesses the recoverable deformation and stiffness of compacted soils. Several mathematical models estimate *RM* parameters, considering different factors: confining stress (Biarez, 1962), stress invariant (Yoder and Witczak, 1975), deviatoric stress (Svenson, 1980), a combined model incorporating both stresses (Pezo et al., 1992), and the universal model, which accounts for stress invariants and octahedral shear stress (AASHTO, 2004). The coefficient of determination (R^2) is used to evaluate model performance. Table 2 presents the mathematical models applied in the analysis.

Due to limited material availability, triplicate *RM* tests were not conducted. However, during compaction curve preparation, the available specimens underwent triaxial testing, enabling *RM* analysis under different moisture conditions. The materials failed to withstand testing at moisture levels beyond *OMC* on the wet side of the compaction curve. The tested moisture conditions for each soil were: (i) Soil 1: -2% of *OMC* (31.0%) and *OMC* (33.0%); (ii) Soil 2: -2% of *OMC* (8.7%) and *OMC* (10.7%); (iii) Soil 3: -4% of *OMC* (13.0%), -2% of *OMC* (15.0%), and *OMC* (17.0%).

3.3 *PD* analysis

Several models exist for predicting *PD* in soils and granular materials, including Barksdale (1972), Monismith et al. (1975), and Tseng & Lytton (1989). However, considering the location of materials, the expansion of the Brazilian soil database, and the strong correlation with tropical soil characteristics, this study focuses exclusively on the Guimarães model (Equation 1), with coefficients obtained via the optimized *PD* S method (Guimarães et al., 2018; Lima et al., 2019, 2020, 2021; Mota et al., 2024).

$$\varepsilon_{p(\%)} = \psi_1 \left(\sigma_3 / \rho_a\right)^{\psi_2} . \left(\sigma_d / \rho_a\right)^{\psi_3} . N^{\psi_4} \tag{1}$$

$\varepsilon_{p(\%)}$: plastic specific deformation; ψ_1, ψ_2, ψ_3, ψ_4: parameters experimentally determined; N: number of load application cycles.

The optimized *PD* S method estimates material behavior by incorporating confining stress, the confining-to-deviatoric stress ratio, and the number of loading cycles. This approach is feasible due to the stress-dependent nature of soils and granular materials, influenced by load magnitude and stress ratio. Equations 2-4 define the S parameter, *PD* S, and reduced cycle count (N_{red}), where σ_3 is confining stress (MPa), σ_d is deviatoric stress (MPa), and N is the number of cycles.

Table 2. Mathematical models used to obtain resilient deformation parameters.

Properties	Models	Equation
Resilient Modulus	Confining Stress (Biarez, 1962)	$RM = k_1 . \sigma_3^{k_2}$
	Stress Invariant (Yoder and Witczak, 1975)	$RM = k_1 . \theta^{k_2}$
	Deviatoric Stress (Svenson, 1980)	$RM = k_1 . \sigma_d^{k_2}$
	Compound (Pezo et al., 1992)	$RM = k_1 . \sigma_3^{k_2} . \sigma_d^{k_3}$
	Universal (AASHTO, 2004)	$RM = k_1 . \rho_a \left(\theta / \rho_a\right)^{k_2} . \left(\tau_{oct} / \rho_a + 1\right)^{k_3}$

Where: *RM*: resilient modulus; σ_3: confining stress; σ_d: deviatoric stress; θ: principal stress; τ_{oct}: octahedral stress; ρ_a: atmospheric pressure; k_1, k_2 *e* k_3: resilient parameters experimentally determined.

$$S = \left(\frac{\sigma_3}{0,04}\right)^{s_1} \times \left(\frac{\sigma_d}{\sigma_3}\right)^{s_2} \tag{2}$$

$$PD\,S = a_1 \times S^{a_2} \times N^{a_3} \tag{3}$$

$$N_{red} = N \times SF \tag{4}$$

The coefficients s_1 and s_2 (S parameter) and a_1, a_2 e a_3 (*PD* S) are determined through an iterative process minimizing the mean square error (MSE) between laboratory test results and model predictions. Similar to master curves for asphaltic materials, where a reference temperature is selected, the method described by Mota et al. (2024) defines a reference stress pair, alinging the remaining pairs using Shift Factors (*SF*) to create a unified master curve. In this shifting process, curves for stress pairs with a ratio $\sigma_3/\sigma_d > 1/2$ shift left, while those with $\sigma_3/\sigma_d < 1/2$ shift right. This adjustment is necessary as more severe stress pairs (e.g., 1/3 ratio) represent *PD* behavior for higher cycle counts in a lower stress ratio pair.

The *PD* S method reduces load cycles to 10,000 for five stress pairs (40/40, 80/80, 40/120, 120/240, and 80/240) while maintaining 150,000 cycles only for the most severe stress pair (120/360). This reduction is enabled by the overlap of points from different stress pairs after shifting, eliminating redundant data points and streamlining the analysis. If the material cannot withstand the 120/360 stress pair, the next less severe pair is tested up to 150,000 cycles. Once the master curves are constructed and *PD* values obtained, the Guimarães (2009) model coefficients are derived for use in mechanistic-empirical pavement design software, such as FlexPaveBR.

3.4 Shakedown theory

The shakedown behavior was assessed using the Werkmeister et al. (2001) model. Permanent deformation results were analyzed by correlating accumulated vertical deformation with its rate of increase per load cycle, classifying materials into Level A (shakedown), B (plastic creep), C (incremental collapse), or AB (initial high deformation followed by stabilization). The AB classification was adapted for Brazilian soils by Guimarães (2009).

3.5 Mechanistic-empirical simulations

With the parameters from the Guimarães model obtained through the master curves and considering the average *RM* of the material, simulations of a typical road pavement structure were conducted using the FlexPaveBR software. In FlexPaveBR, it is currently only possible to use the average *RM* of the material. For this purpose, the following conditions were considered:

- Intermediate traffic (*N*: 5×10^6) and heavy traffic (2×10^7) (Ceratti et al., 2015);
- Failure criteria of maximum of 12.5 mm of rutting to the end of pavement life;
- Equivalent single axle load of 8.2 tf and tire pressure of 0.83 MPa;
- Design period of 10 years with average growth rate of 3.0%.

The pavement structure considered in the analysis comprises 5 cm of asphalt concrete (Class 3, *RM*: 8000 MPa) and 15 cm of a granular material base (*RM*: 381 MPa). A 15 cm thick subbase layer composed of the three materials evaluated in this study was also considered. The subgrade material consisted of a silty soil classified as NS', with a *RM* of 189 MPa. The materials and conditions were considered in the simulations performed using FlexPaveBR, version 2.1.5. It is important to note that, although the DNIT method (2006) recommends an asphalt concrete thickness of 10 cm for heavy traffic, a reduced thickness of 5 cm was adopted in this study. This choice aimed to emphasize the contribution of the granular layer, composed of the studied soils, to the pavement response.

4. Results

4.1 Resilient modulus

The elastic modulus results were evaluated using five *RM* predictive models through multiple nonlinear regression for each testing condition. Each tested specimen generated 18 modulus values, corresponding to the applied stress pairs. Figure 2 illustrates the variation of *RM* concerning confining and deviatoric stresses, along with changes in moisture content. Table 3 presents the parameters derived from these *RM* values for each specimen condition. None of the specimens withstood testing under the condition of +2% above the *OMC*, even when evaluated using subgrade material criteria. Both materials exhibited permanent deformation exceeding 10 mm during the conditioning phase, which prevented the continuation of the test.

The Universal (AASHTO, 2004) and Compound (Pezo et al., 1992) models best represented the seven groups of samples, as both consider the combined influence of confining and deviatoric stresses. In the Compound model, *RM* increases with rising confining stress but decreases as deviatoric stress increases. Models that evaluate these stresses individually, as well as those based on stress invariants, did not adequately represent the samples, except for Soil 1 at *OMC*, where the Svenson model captured the resilient behavior reasonably well, though it did not achieve the highest R^2 value.

Soil 2 at *OMC* exhibited low R^2 values across all five evaluated models, indicating that classical formulations do not adequately capture its behavior. This may be attributed to its mixed composition of 73% sand and 26% clay, along with its high sensitivity to moisture, a factor not accounted for in these models. Additionally, the internal structure and potential partial cementation - common in tropical soils - may contribute to nonlinear and inelastic responses, making model fitting more challenging. Another influencing factor is the significant *PD* observed during the conditioning phase, which likely introduced transient responses that were not well captured by models based solely on elastic behavior. During conditioning, Soil 2 at *OMC* exhibited 5.06 mm of *PD* and accumulated an additional 0.33 mm during the *RM* test, resulting in a total *PD* of 5.39 mm. This behavior can be explained by the fact that Soil 2 was compacted at a higher energy, thus reducing the voids in the soil and resulting in greater initial settlement.

Figure 2 shows that *RM* decreases as moisture content increases and increases as moisture decreases. It is important to emphasize that, although the materials exhibited satisfactory performance under moisture conditions below the *OMC*, it is essential to conduct post-compaction moisture variation studies. Soils with higher *PI*, such as Soil 1 (*PI* = 26%), displayed greater sensitivity to moisture variations, leading to more pronounced *RM* fluctuations. However, for lower deviatoric stresses, *RM* was higher at *OMC* compared to -2% *OMC* for Soil 2, a trend also observed when analyzing *RM* variation with confining stress. Only beyond a certain applied stress threshold did *RM* become higher under lower moisture conditions.

This behavior can be explained by the effects of matric suction. When the soil is dry (below *OMC*), it exhibits higher suction and may have weak or incomplete particle bonds, which hinder elastic deformation and limit effective stress transmission. Under low stress conditions, suction dominates, making the soil locally stiffer but restricting stress redistribution, resulting in a reduced initial *RM*. In contrast, at *OMC*, the soil contains an optimal water content that lubricates particle contacts, facilitating elastic accommodation without structural collapse. Consequently, *RM* is higher under low stress conditions at *OMC*, aligning with findings from Khoury et al. (2009) and Pascoal (2024). In this study, suction was not determined; however, it is important to include such determinations in future research.

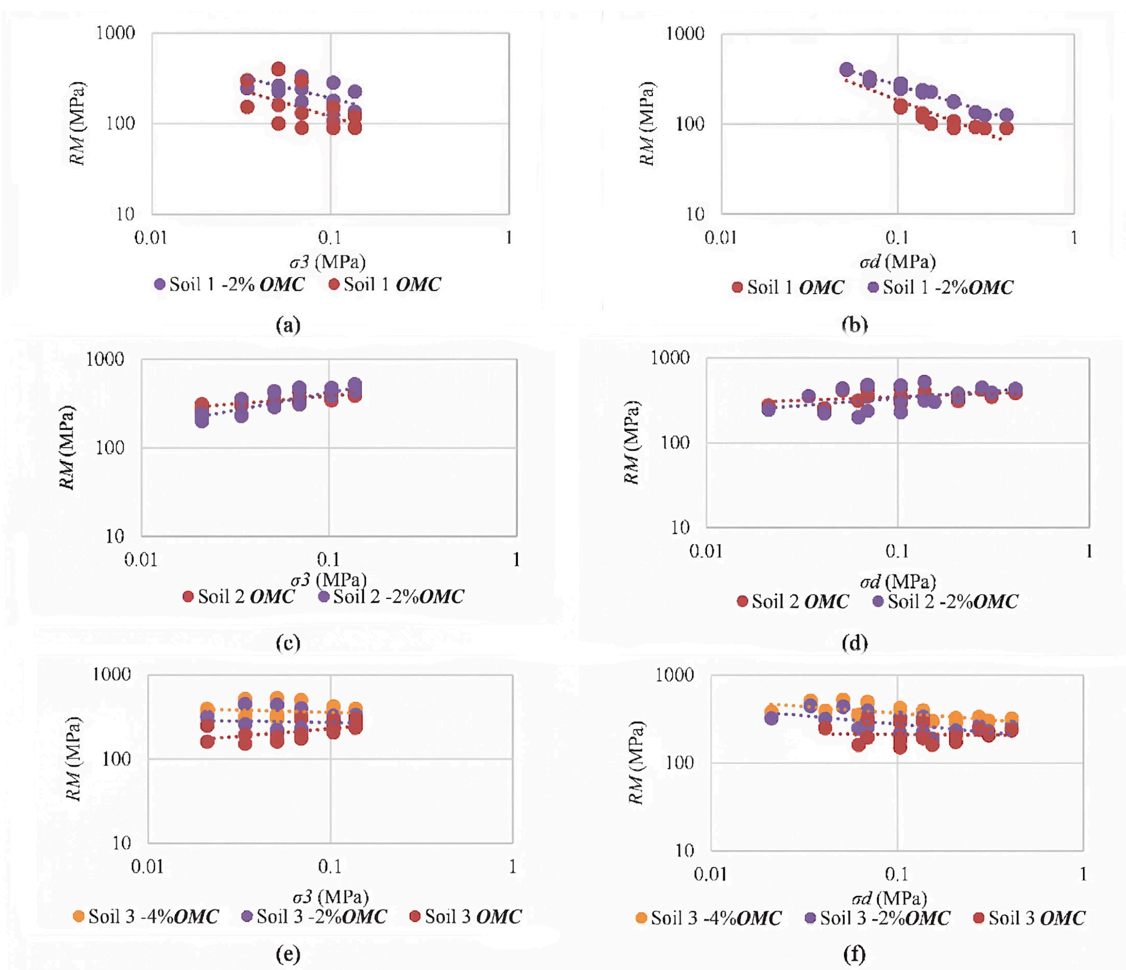

Figure 2. Variation of *RM* with confining and deviatoric stress. (a) Soil 1 with σ_3. (b) Soil 1 with σ_d. (c) Soil 2 with σ_3. (d) Soil 2 with σ_d. (e) Soil 3 with σ_3. (f) Soil 3 with σ_d.

Table 3. Resilient parameters for five mathematical models.

Soil	Condition	Model	k_1	k_2	k_3	R^2	*RM* avg (MPa)
Soil 1	-2% of the *OMC*	Confining Stress	65.18	-0.467	-	0.32	234
		Stress Invariant	118.08	-0.626	-	0.63	
		Deviatoric Stress	69.73	-0.585	-	0.97	
		Compound	81.74	0.080	-0.613	0.97	
		Universal	4897.47	0.099	-1.756	0.95	
	OMC	Confining Stress	31.24	-0.584	-	0.26	163
		Stress Invariant	61.15	-0.792	-	0.57	
		Deviatoric Stress	33.23	-0.744	-	0.89	
		Compound	17.33	0.026	-1.071	0.94	
		Universal	7345.09	-0.056	-3.268	0.87	
Soil 2	-2% of the *OMC*	Confining Stress	1051.80	0.397	-	0.70	352
		Stress Invariant	509.89	0.325	-	0.49	
		Deviatoric Stress	497.41	0.171	-	0.18	
		Compound	1153.85	0.641	-0.271	0.91	
		Universal	2654.82	0.753	-1.162	0.78	
	OMC	Confining Stress	574.23	0.173	-	0.52	356
		Stress Invariant	421.39	0.147	-	0.37	
		Deviatoric Stress	423.47	0.083	-	0.14	
		Compound	602.00	0.293	-0.132	0.68	
		Universal	3194.41	0.381	-0.686	0.59	
Soil 3	-4% of the *OMC*	Confining Stress	315.77	-0.055	-	0.03	375
		Stress Invariant	321.43	-0.109	-	0.14	
		Deviatoric Stress	262.68	-0.150	-	0.39	
		Compound	397.49	0.303	-0.352	0.74	
		Universal	4715.60	0.301	-1.232	0.62	
	-2% of the *OMC*	Confining Stress	249.76	-0.036	-	0.01	287
		Stress Invariant	238.13	-0.119	-	0.10	
		Deviatoric Stress	179.69	-0.191	-	0.35	
		Compound	327.48	0.465	-0.515	0.76	
		Universal	3912.70	0.393	-1.651	0.49	
	OMC	Confining Stress	347.21	0.180	-	0.23	217
		Stress Invariant	241.44	0.117	-	0.08	
		Deviatoric Stress	205.53	-0.015	-	0.01	
		Compound	358.01	0.502	-0.424	0.78	
		Universal	2057.41	0.563	-1.219	0.49	

4.2 Permanent deformation

The *PD* tests were conducted at intermediate energy for Soils 1 and 3 and at modified energy for Soil 2, all compacted at their respective *OMC*. The tests followed the number of blows and stress pairs recommended by Mota et al. (2024) for obtaining the master curves of the materials. Figure 3 presents the *PD* (%) versus N_{red} (150,000 cycles) based on the master curves, while Figure 4 displays the *PD* (%) versus N_{red} curves formatted according to DNIT 179 (2018b), also derived from the master curves.

From Figure 3, it is possible to determine up to which value of N_{red} the *PD* can be estimated for each stress pair, as well as the influence of each stress pair on the master curve and the corresponding *PD* increments. Figure 4 demonstrates that as applied stresses increase, *PD* also rises, while with an increasing number of load cycles, deformations tend to stabilize. The graphs in Figure 4 are related to the final values predicted by the Guimarães (2009) model, obtained using the master curves. Higher stress levels are generally associated with thinner pavement structures, where traffic-induced stresses reach deeper layers, affecting the subgrade more significantly.

As expected, the highest permanent deformation occurred under the most severe stress pair (120/360) due to its magnitude, except for Soil 1, which exhibited plastic rupture at the 80/240 stress pair. As deviatoric stress increases, *PD* also intensifies; however, with a higher number of load cycles, the rate of *PD* accumulation decreases. The final deformation of specimens subjected to the most severe stress pair for each soil was 13.54 mm for Soil 1 (80/240 stress pair, 5,000 cycles),

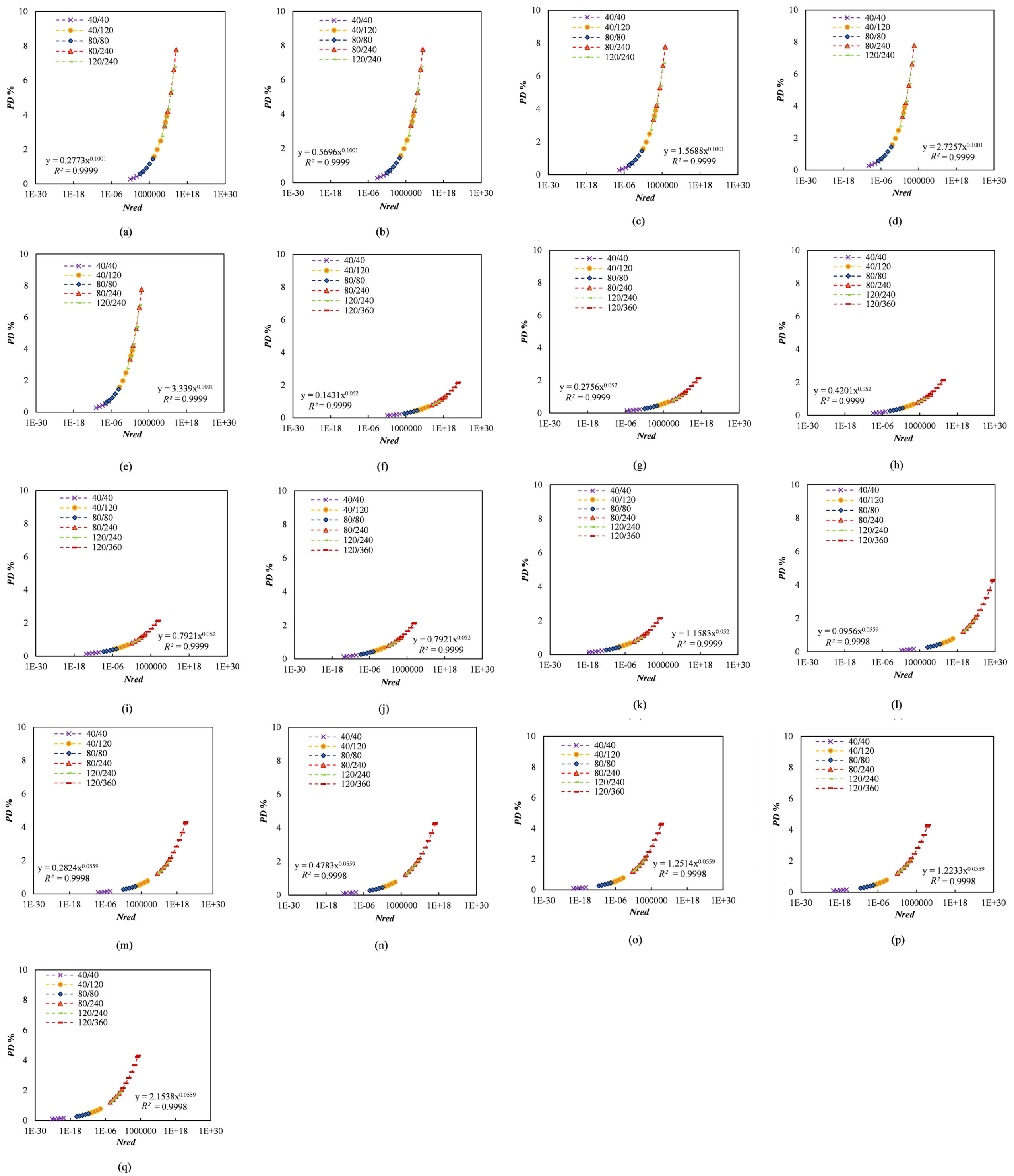

Figure 3. Master curves for each stress pair (a) 40/40 (Soil 1); (b) 80/80 (Soil 1); (c) 40/120 (Soil 1); (d) 120/240 (Soil 1); (e) 80/240 (Soil 1); (f) 40/40 (Soil 2); (g) 80/80 (Soil 2); (h) 40/120 (Soil 2); (i) 120/240 (Soil 2); (j) 80/240 (Soil 2); (k) 120/360 (Soil 2); (l) 40/40 (Soil 3); (m) 80/80 (Soil 3); (n) 40/120 (Soil 3); (o) 120/240 (Soil 3); (p) 80/240 (Soil 3); and (q) 120/360 (Soil 3). Note: Soil 1 failed by plastic rupture under the 80/240 stress pair.

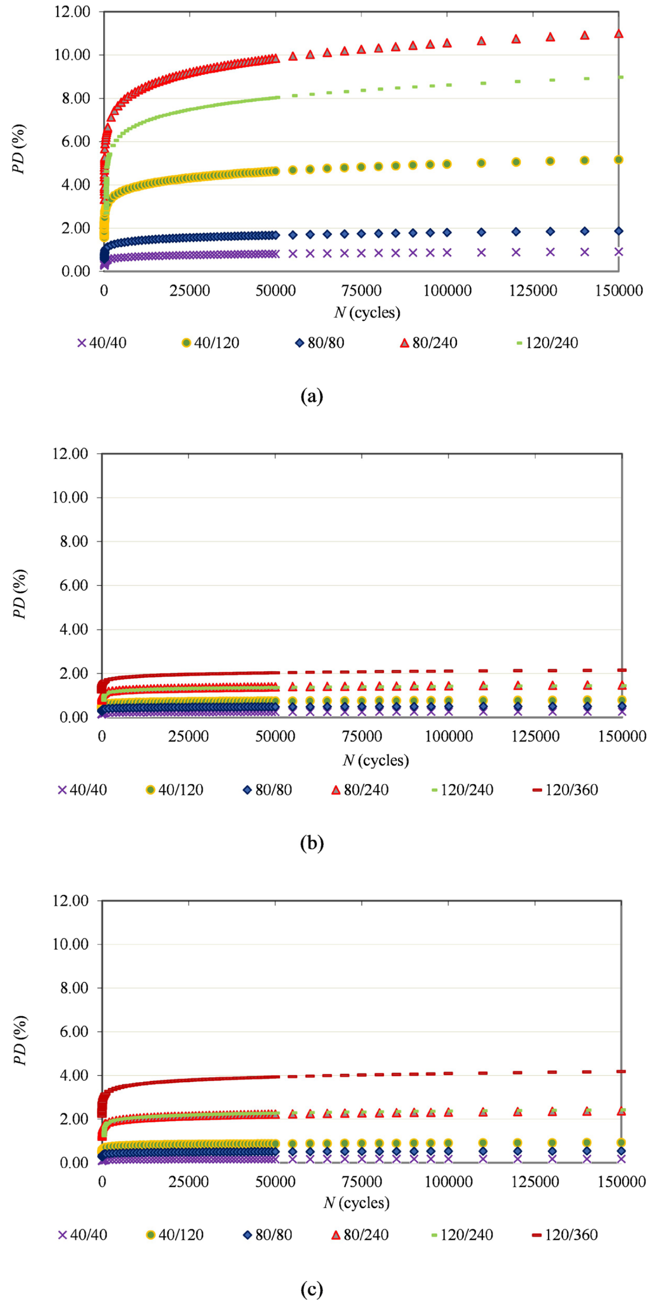

Figure 4. Predicted Accumulated Permanent Deformation of (a) Soil 1, (b) Soil 2, and (c) Soil 3.

4.08 mm for Soil 2 (120/360 stress pair, 150,000 cycles), and 7.94 mm for Soil 3 (120/360 stress pair, 150,000 cycles).

As expected, the highest permanent deformation occurred under the most severe stress pair (120/360) due to its magnitude, except for Soil 1, which exhibited plastic rupture at the 80/240 stress pair. As deviatoric stress increases, *PD* also intensifies; however, with a higher number of load cycles, the rate of *PD* accumulation decreases. The final deformation of specimens subjected to the most severe stress pair for each soil was 13.54 mm for Soil 1 (80/240 stress pair, 5,000 cycles), 4.08 mm for Soil 2 (120/360 stress pair, 150,000 cycles), and 7.94 mm for Soil 3 (120/360 stress pair, 150,000 cycles).

Due to material limitations, no other stress pair for Soil 1 was tested up to 150,000 cycles, as 28 kg of material was required solely for obtaining the compaction curve. However, this constraint did not impact the generation of the master curves, as this material is primarily used as embankment fill. The master curves enabled a 70% reduction in *PD* testing time, as the first five stress pairs were conducted up to 10,000 cycles. To reinforce the findings of Mota et al. (2024), it was observed that after a certain number of loading cycles, deformations tend to stabilize, exhibiting only minor variations. To further investigate this behavior, Figure 5 presents the total deformation for each specimen at 1, 100, 1,000, 10,000, 50,000, and 150,000 cycles for Soils 2 and 3, which were tested up to 150,000 cycles under the 120/360 stress pair. By 10,000 cycles, both soils had already accumulated more than 90% of the *PD* for the most severe stress pair, reinforcing the validity of adopting this value in the construction of master curves.

The impact of higher stress levels on *PD* response is evident. For most materials, the stress pairs follow the σ_3/σ_d ratio sequence of 1/1, 1/2, and 1/3, except for the 40/120 stress pair (1/3 ratio), which appears immediately after the 1/1 ratio pairs due to its low confining and deviatoric stresses. The master curves also highlight the magnitude of deformation for each stress pair. In the initial pairs, deformation amplitude is lower; however, from the 120/240 stress pair onward, *PD* increases significantly over a shorter N_{red} range.

Additionally, greater *PD* variation is observed in the early cycles across all materials and stress pairs. For the most severe stress pair, a shift in slope and direction occurs in the final cycles, further indicating *PD* stabilization. The results also reveal distinct material behaviors under different stress pairs, though *PD* values for the 120/240 and 80/240 stress pairs were very similar for Soils 2 and 3. This behavior is likely due to their higher sand content, demonstrating that greater confining stress contributes to increased *PD* when subjected to the same high deviatoric stress, aligning with findings by Guimarães (2001).

Soil 1 exhibited the highest deformability, failing due to plastic rupture under the 80/240 stress pair. Its high clay content and elevated *OMC* may have led to suction reduction due to moisture introduced during testing, resulting in structural loss, evidenced by plastic flow and progressive failure. The need for eight specimens to obtain the compaction curve further highlights its high sensitivity to moisture variation. This behavior is attributed to the high concentration of silicon and aluminum, suggesting the presence of clay minerals with high water absorption capacity. In contrast, Soils 2 and 3, with higher sand content and lower plasticity, failed at higher stress levels due to the greater mechanical resistance provided by their quartz grains.

Soil 2 demonstrated the best *PD* performance. Despite its similar physical characteristics to Soil 3, its compaction under modified energy resulted in better particle interlocking, increasing specimen stiffness. Using the *PD* values and load application cycles, the rate of *PD* variation was determined, and graphs were generated to assess shakedown conditions, as shown in Figure 6. The material is considered in a shakedown state if its *PD* increase rate reaches approximately $10^{-7} \times 10^{-3}$ meters per load application cycle (Werkmeister et al., 2001). Since only 10,000 cycles per stress pair were tested, this rate was not reached in most cases. However, the curve clearly trends toward alignment parallel to the y-axis, indicating material accommodation, as discussed by Werkmeister et al. (2001) and Guimarães (2009).

Although the curves did not reach the threshold defining shakedown, all, except the 80/240 stress pair of Soil 1 (Type B) and 120/360 stress pair of Soil 2 (Type B), exceeded a rate of $10^{-5} \times 10^{-3}$, classifying them as shakedown behavior Types A or AB. Reducing the number of cycles below 10,000 would prevent a more accurate analysis of whether shakedown has occurred.

The data from each soil set were analyzed using non-linear regression to determine the parameters of the Guimarães (2009) model. Table 4 presents the obtained parameters, considering a ρ_a value of 0.1 MPa and incorporating all *PD* values with their respective stress pairs and load repetition cycles. The coefficients of determination confirmed that

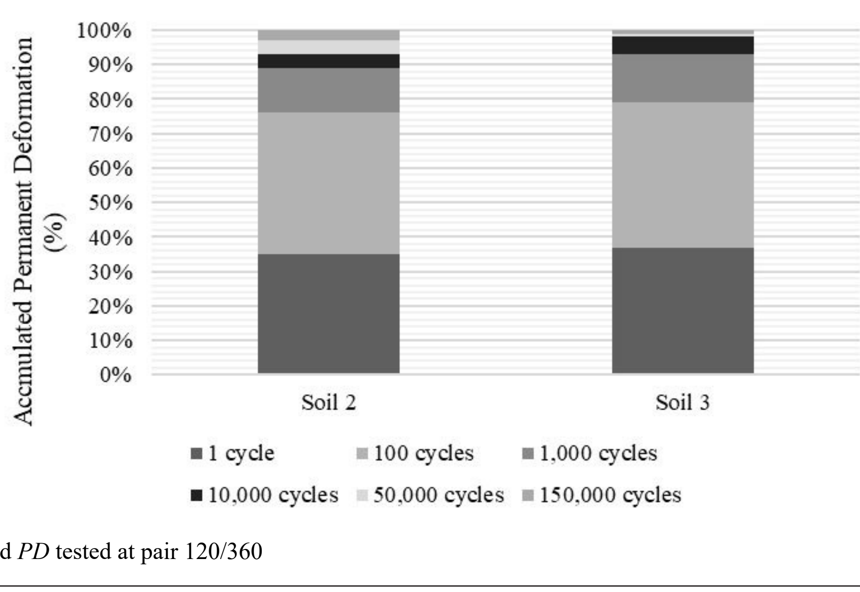

Figure 5. Accumulated *PD* tested at pair 120/360

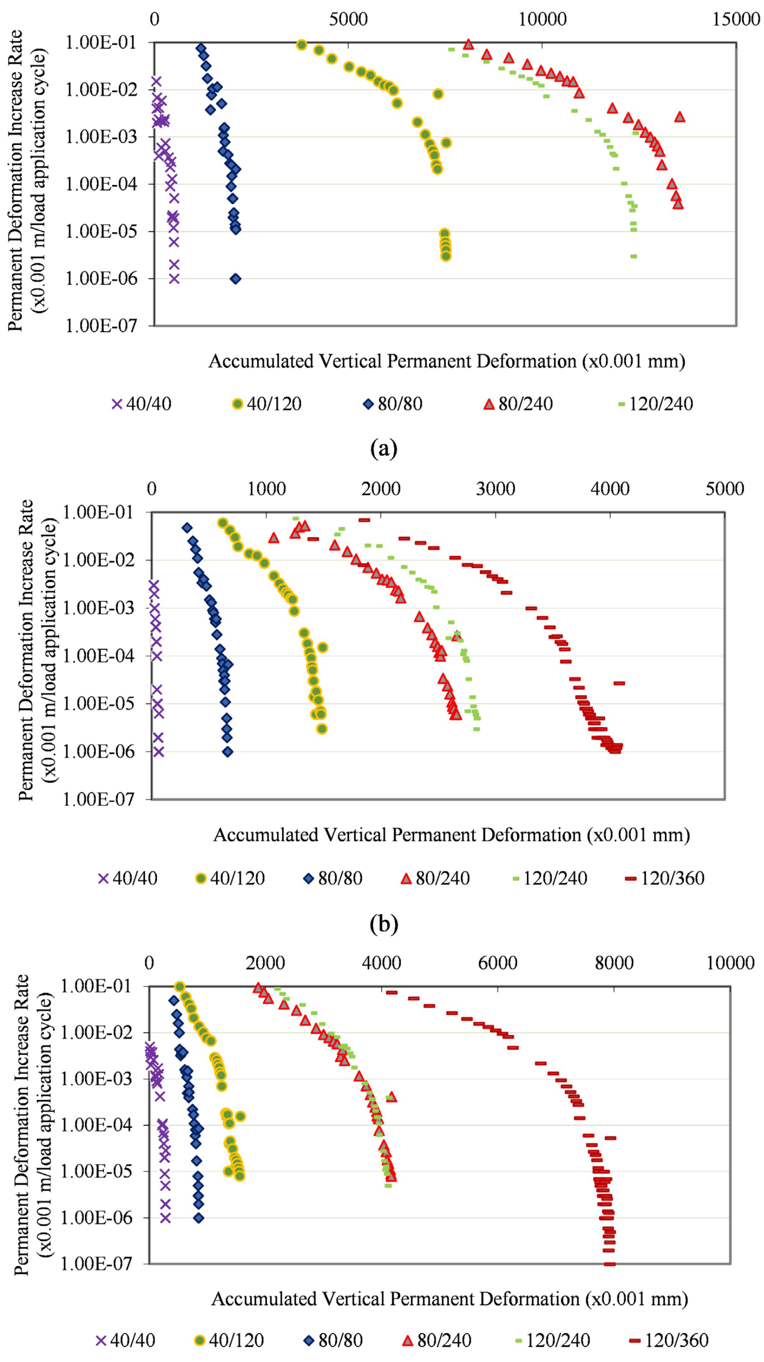

Figure 6. Shakedown curves for (a) Soil 1, (b) Soil 2 and (c) Soil 3

Table 4. Parameters of permanent deformation by the Guimarães model (2009).

Soil	Ψ_1	Ψ_2	Ψ_3	Ψ_4	R^2
1	0.7372	-0.5050	1.5975	0.1001	0.96
2	0.3376	-0.0426	0.9702	0.0520	0.96
3	0.3828	0.0414	1.3424	0.0559	0.95
Software Parameters					
Base	0.0868	-0.2801	0.8929	0.0961	-
Subgrade	0.2440	0.4190	1.3090	0.0690	-

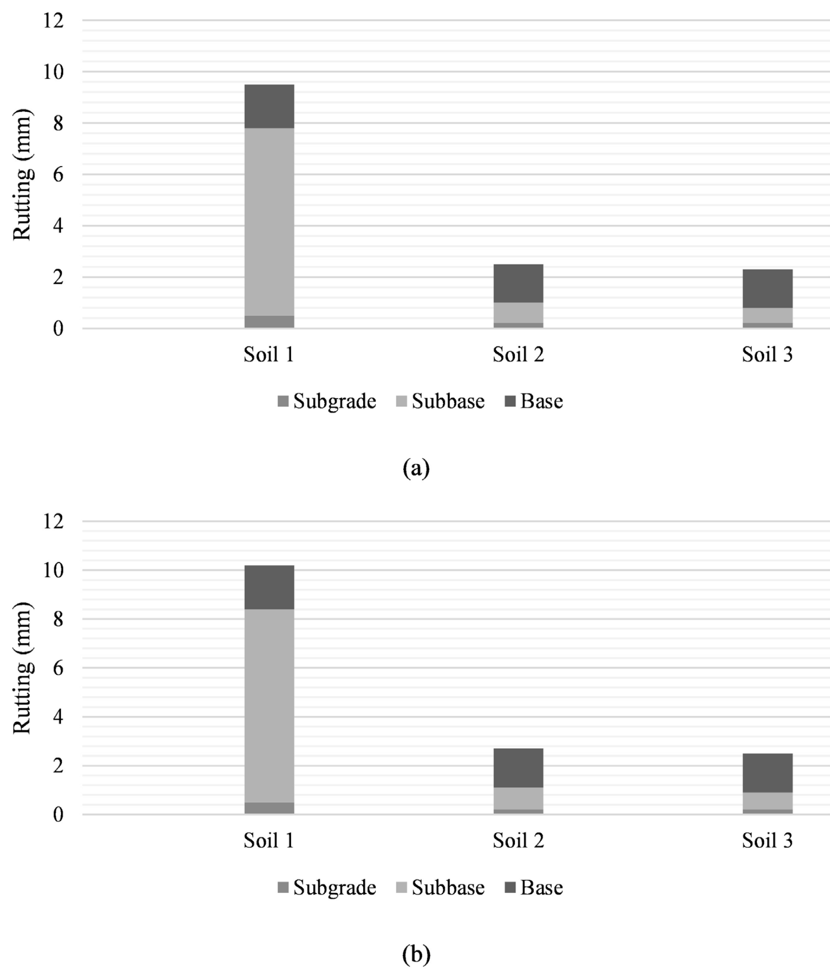

Figure 7. Rutting results for the three soils under (a) intermediate traffic and (b) heavy traffic.

the model adequately represented the deformability of the studied materials.

The coefficient Ψ_2 indicates that for Soils 1 and 2, a decrease in confining stress leads to an increase in *PD*, whereas for Soil 3, an increase in confining stress results in a proportional rise in *PD*. The deviatoric stress, represented by Ψ_3, is consistently positive, with Soil 1 being the most affected by its increase. These findings align with the trends observed in Figure 3, where Soil 2 exhibited the lowest *PD* values and had the smallest coefficient associated with deviatoric stress. The coefficient Ψ_4 reflects sensitivity to the number of load cycles, with Soil 1 displaying a value nearly twice as high as the other two soils, indicating greater susceptibility to traffic-induced deformation.

4.3 Analysis with de Brazilian pavement design method

Figure 7 presents the rutting simulation results for the three soils used as the subbase layer. The simulations were performed using the FlexPaveBR software.

From Figure 7, it is evident that Soil 1 is unsuitable as a subbase material due to its high *PD*, which results in excessive rutting. Conversely, Soils 2 and 3 exhibited good performance as a pavement subbase under the tested traffic conditions. Soil 2 showed a maximum rutting of 0.9 mm, while Soil 3 reached a maximum of 0.7 mm.

Overall, despite being classified by AASHTO as having poor to very poor behavior, Soils 2 and 3 performed well as subbase materials, benefiting from the well-defined properties of tropical soils characterized by the MCT classification. The Brazilian national pavement design method sets a 5% deformation limit per layer relative to its final thickness. Based on this criterion, Soils 2 and 3 met the requirements, whereas Soil 1 was deemed unsuitable. However, granulometric or chemical stabilization could result in better mechanical properties.

5. Final considerations

This study aimed to characterize the elastic and plastic behavior of three soils from the metropolitan region of Manaus, evaluate their performance, and assess their suitability for use in pavement layers, despite their classification as poor to very poor according to AASHTO. The key findings were:

- Based on the MCT classification, the soils were identified as NG', LA', and LG'. Two of the three materials were deemed suitable for pavement applications, provided they were properly characterized. EDXRF testing confirmed the predominance of silicon dioxide, iron oxide, and aluminum oxide, aligning with the MCT classification. However, Soil 1 exhibited high plasticity and water absorption capacity, negatively affecting its plastic behavior.
- Regarding resilient behavior, the Compound and Universal models showed the best correlations. *RM* decreased significantly with increasing moisture content. However, due to the suction effect in more plastic soils, the opposite trend was observed at lower stress levels, where *RM* at *OMC* exhibited higher values.
- The analyzed materials exhibited stabilization in *PD*, classifying as Type I or II. The master curves were effective in determining the parameters for the Guimarães (2009) model, which showed strong correlations in representing soil deformability. Notably, for the most severe stress pair of Soils 2 and 3, approximately 90% of *PD* accumulated within the first 10,000 cycles, as defined by the optimized *PD* method by Mota et al. (2024) for lower stress pairs.
- In assessing shakedown behavior, all samples exhibited plastic accommodation tendencies, but some did not reach the *PD* rate required by Brazilian standards. Most samples demonstrated Type A behavior, indicating minimal soil contribution to surface rutting. However, Soil 1 under the 80/240 stress pair and Soil 2 under the 120/360 stress pair exhibited Type B behavior, indicative of plastic failure.
- The *PD* model was effectively represented in mechanistic-empirical simulations using FlexPaveBR, yielding rutting results consistent with laboratory-measured *PD* behavior. Simulations for two different N values confirmed the feasibility of using these materials in subbase layers, particularly regarding plastic settlement.

This study contributed to the development of a simplified method for analyzing *PD* and *RM* of fine soils from the Manaus region, achieving a reduction in testing time of up to 70%, when compared to the method of the DNIT 179 standard (2018), without compromising result accuracy. Additionally, it advanced the understanding of the chemical properties of plastic soils and their application in pavement construction.

Practically, using these soils as subbase materials in the Amazon can lower costs, given the scarcity of high-quality aggregates and the long transport distances from quarries. Reusing local fine soils also reduces environmental impacts and supports sustainability. Although their performance is below that of crushed stone, mechanistic-empirical simulations confirm their suitability for low- to medium-traffic roads, especially where economic and environmental constraints are decisive.

The findings contribute directly to ongoing updates of Brazilian pavement design methods by reinforcing the relevance of MCT classification and mechanistic-empirical calibration for fine tropical soils. Internationally, this approach may also support pavement design in other tropical regions where conventional classification systems underestimate the potential of fine lateritic soils.

A limitation of this study is the absence of direct matric suction measurements, although their influence was indirectly observed through inverse *RM* trends in plastic soils at lower stress levels. Future research should quantify matric suction and correlate it with *RM* and *PD* to better explain moisture sensitivity in fine-grained tropical soils and to improve the predictive capacity of *RM* models. It should also investigate the effect of chemical or granulometric stabilization techniques on soils that did not exhibit satisfactory mechanical performance, particularly for Soil 1. Future studies should also include field validation in experimental tracks or actual roadway sections in the Amazon region. This would enable the calibration of the proposed laboratory-based models with real traffic and climate conditions, ensuring broader applicability of the results. These processes can benefit society by promoting the rational use of materials and the efficient utilization of natural resources.

Acknowledgements

The authors acknowledge the financial support received from Cenpes/Petrobras, the National Petroleum Agency (ANP) through PRH-4 and Process No. 2024/11269-5 of the São Paulo Research Foundation (Fapesp), the Brazilian Coordination for the Improvement of Higher Education Personnel (Capes) - Finance Code 001, and the National Council for Scientific and Technological Development (CNPq).

Declaration of interest

The authors have no conflicts of interest to declare. All co-authors have observed and affirmed the contents of the paper and there is no financial interest to report.

Authors' contributions

Bruno Cavalcante Mota: conceptualization, data curation, visualization, methodology, and experimental procedures, writing - original draft, review & editing. Mariluce de Oliveira Ubaldo: study planning, data curation, experimental procedures, writing - review. Daniela Muniz D'Antona Guimarães: study planning, data collection, validation, writing - review. Caroline Dias Amancio de Lima: study planning, validation, writing - review. Lilian Ribeiro de Rezende: study planning, validation, writing - review. Luis

Alberto Herrmann do Nascimento: supervision, writing - review. Francisco Thiago Sacramento Aragão: supervision, funding acquisition, project administration, writing - review.

Data availability

All data produced or examined in the course of the current study are included in this article.

Declaration of use of generative artificial intelligence

This manuscript benefited from the assistance of ChatGPT, which was used solely to improve the clarity and quality of the writing. No content was generated by the tool. All aspects of the manuscript were developed solely by the authors, who take full responsibility for the content of this publication.

List of symbols and abbreviations

k_1, k_2, k_3	Resilient parameters experimentally determined
w_L	Liquid limit
w_P	Plastic limit
AASHTO	American Association of State Highway and Transportation Officials
ABNT	Brazilian Association of Technical Standards
Al	Aluminum
AM	Amazonas
ANP	National Petroleum Agency
Capes	Brazilian Coordination for the Improvement of Higher Education Personnel
CBR	California bearing ratio
Cenpes	Leopoldo Américo Miguez de Mello Research and Development Center
CNPq	National Council for Scientific and Technological Development
Coppe	Alberto Luiz Coimbra Institute for Graduate Studies and Engineering Research
DNIT	National Department of Transportation Infrastructure
EDXRF	Energy Dispersive X-ray Fluorescence
Fapesp	São Paulo Research Foundation
Fe	Iron
IE	Intermediate energy
LA’	Lateritic sandy
LG’	Lateritic clayey
LVDT	Linear Variable Differential Transformer
MCT	Miniature, Compacted, Tropical
MDD	Maximum dry density
ME	Modified energy
MSE	Mean square error
N	Number of loading cycles
NCSU	North Caroline State University
NG’	Non-lateritic clay
N_{red}	Reduced number of loading cycles
OMC	Optimum moisture content
PD	Permanent deformation
PI	Plasticity Index
PPEC	Graduate Program in Civil Engineering
PPG-GECON	Graduate Program in Geotechnics, Structures, and Civil Engineering
R^2	Coefficient of determination
RM	Resilient modulus
SF	Shift Factors
Ti	Titanium
UFRGS	Federal University of Rio Grande do Sul
UFRJ	Federal University of Rio de Janeiro
USCS	Unified Soil Classification System
ε_p	Specific permanent deformation
θ	Principal stress
ρ_a	Atmospheric pressure
σ_3	Confining stress
σ_d	Deviatoric stress
σ_3 / σ_d	Stress ratio
τ_{oct}	Octahedral stress
ψ_n	Permanent deformation parameters experimentally determined

References

AASHTO NCHRP 1-37A. (2004). *Guide for mechanistic-empirical design of new and rehabilitated pavement structures - Final Report.* Transportation Research Board, Washington, D.C.

ABNT NBR 7180. (2016a). *Determinação do limite de plasticidade.* ABNT - Associação Brasileira de Normas Técnicas, Rio de Janeiro, RJ (in Portuguese).

ABNT NBR 7181. (2016b). *Solo - Análise granulométrica.* ABNT - Associação Brasileira de Normas Técnicas, Rio de Janeiro, RJ (in Portuguese).

ABNT NBR 6459. (2016c). *Solo - Determinação do limite de liquidez.* ABNT - Associação Brasileira de Normas Técnicas, Rio de Janeiro, RJ (in Portuguese).

Araújo, M.J.R., Barroso, S.H.A., Ribeiro, A.J.A., & Vieira, F.A.F. (2024). Definition of new stopping criteria for the characterization of permanent deformation of granular materials. *Transportation Geotechnics*, *44*, 101159. http://doi.org/10.1016/j.trgeo.2023.101159.

Barksdale, R.D. (1972). Laboratory evaluation of rutting in base course materials. In *Conference on the Structural Design of Asphalt Pavements* (pp. 161-174), London, England.

Bernucci, L.B., Motta, L.M.G., Ceratti, J.A.P., & Soares, J.B. (2022). *Pavimentação asfáltica: formação básica para engenheiros* (2. ed.). Petrobras; Abeda.

Biarez, J. (1962). *Contribution a l’étude des proprietes mecaniques des sols et des materiaux pulverents* [Doctoral thesis]. Faculté des Sciences.

Cabral, W.S., Barroso, S.H.A., & Silva, S.A.T. (2021). Consideração da deformação permanente de solos ocorridos na região nordeste na análise mecanística-empírica de pavimentos. *Matéria*, 26(4), e13096. http://doi.org/10.1590/s1517-707620210004.1396.

Ceratti, J.A., Bernucci, L.B., & Soares, J.B. (2015). *Utilização de ligantes asfálticos em serviços de pavimentação*. Abeda.

Cerni, G., Cardone, F., Virgili, A., & Camilli, S. (2012). Characterisation of permanent deformation behaviour of unbound granular materials under repeated triaxial loading. *Construction & Building Materials*, 28(1), 79-87. http://doi.org/10.1016/j.conbuildmat.2011.07.066.

Dawson, A.R., & Wellner, F. (1999). *Plastic behavior of granular materials – Report ARC Project 933, Reference PRG 99014*. University of Nottingham.

Departamento Nacional de Infraestrutura de Transportes – DNIT. (2006). *Manual de pavimentação*. Instituto de Pesquisas em Transportes.

DNIT 134. (2018a). *Pavimentação - Solos - Determinação do modulo de resiliência - Método do ensaio.* IPR - Instituto de Pesquisas em Transportes, Rio de Janeiro, RJ (in Portuguese).

DNIT 179. (2018b). *Pavimentação - Solos - Determinação da deformação permanente - Instrução do ensaio.* IPR - Instituto de Pesquisas em Transportes, Rio de Janeiro, RJ (in Portuguese).

DNIT 258. (2023a). *Solos - Compactação em equipamento miniatura - Ensaios Mini-MCV e perda de massa por imersão - Método de ensaio.* IPR - Instituto de Pesquisas em Transportes, Rio de Janeiro, RJ (in Portuguese).

DNIT 259. (2023b). *Solos - Classificação de solos finos tropicais para finalidades rodoviárias utilizando corpos de prova compactados em equipamento miniatura - Classificação.* IPR - Instituto de Pesquisas em Transportes, Rio de Janeiro, RJ (in Portuguese).

DNIT 444. (2023c). *Classificação de solos tropicais de granulação grossa - Classificação.* IPR - Instituto de Pesquisas em Transportes, Rio de Janeiro, RJ (in Portuguese).

Falesi, I.C. (1972). *O estado atual dos conhecimentos sobre os solos da Amazônia Brasileira* (Boletim Técnico, No. 54, pp. 17-67). Instituto de Pesquisas e Experimentação Agropecuárias do Norte.

Guimarães, A.C.R. (2001). *Estudo de deformação permanente em solos e a teoria do Shakedown aplicada a pavimentos flexíveis* [Master dissertation]. Universidade Federal do Rio de Janeiro (in Portuguese).

Guimarães, A.C.R. (2009). *Um método mecanístico-empírico para a previsão da deformação permanente em solos tropicais constituintes de pavimentos* [Doctoral thesis]. Universidade Federal do Rio de Janeiro (in Portuguese).

Guimarães, A.C.R., Motta, L.M.G., & Castro, C.D. (2018). Permanent deformation parameters of fine - grained tropical soils. *Road Materials and Pavement Design*, 20(7), 1664-1681. http://doi.org/10.1080/14680629.2018.1473283.

Huang, Y.H. (2004). *Pavement analysis and design*. 2nd ed. Pearson Prentice Hall.

Khoury, N., Brooks, R., Zaman, M.M., & Khoury, C.N. (2009). Variations of resilient modulus of subgrade soils with postcompaction moisture contents. *Transportation Research Record: Journal of the Transportation Research Board*, 2101(1), 72-81. http://doi.org/10.3141/2101-09.

Kim, I., Tutumluer, E., & Tutumluer, K. (2004) Predicting rutting performance of pavement granular layers at the FAA's National Airport Pavement Test Facility. In *Proceedings of the 2004 FAA worldwide airport technology transfer conference*. Atlantic City, New Jersey, USA.

Lima, H.N., Mello, J.W.V., Schaefer, C.E.G.R., Ker, J.C., & Lima, A.M.N. (2006). Mineralogia e química de três solos de uma topossequência da bacia sedimentar do Alto Solimões, Amazônia Ocidental. *Revista Brasileira de Ciência do Solo*, 30(1), 59-68. http://doi.org/10.1590/S0100-06832006000100007.

Lima, C.D.A., Motta, L.M.G., & Aragão, F.T.S. (2019). Effects of compaction moisture content on permanent deformation of soils subjected to repeated triaxial load tests. *Transportation Research Record: Journal of the Transportation Research Board*, 2673(55), 1-11. http://doi.org/10.1177/0361198118825124.

Lima, C.D.A., Motta, L.M.G., Aragão, F.T.S., & Guimarães, A.C.R. (2020). Mechanical characterization of fine-grained lateritic soils for mechanistic-empirical flexible pavement design. *Journal of Testing and Evaluation*, 48(1), 1-17. http://doi.org/10.1520/JTE20180890.

Lima, C.D.A., Motta, L.M.G., & Aragão, F.T.S. (2021). A permanent deformation predictive model for fine tropical soils considering the effects of the compaction moisture content on material selection. *Transportation Geotechnics*, 28, 100534. http://doi.org/10.1016/j.trgeo.2021.100534.

Lima, L.B.F., Silva, J.P.S., & Rezende, L.R. (2023). Investigation of resilient modulus and permanent deformation of tropical soil with Reclaimed Asphalt Pavement. *Transportation Geotechnics*, 43, 101103. http://doi.org/10.1016/j.trgeo.2023.101103.

Medina, J., & Motta, L.M.G. (2015). *Mecânica dos pavimentos* (638 p.). Editora Interciência.

Monismith, C.L., Ogawa, N., & Freeme, C.R. (1975). Permanent deformation characteristics of subgrade soils due to repeated loading. *Transportation Research Record: Journal of the Transportation Research Board*, (537), 1-17.

Mota, B.C., Ubaldo, M.O., Lima, C.D.A., Nascimento, L.A.H., & Aragão, F.T.S. (2024). Optimized characterization of the permanent deformation of unbound soils and granular materials considering the master curve concept. *Transportation Geotechnics*, 47, 101291. http://doi.org/10.1016/j.trgeo.2024.101291.

Nogami, J.S., Cozzolino, V.M.N., & Villibor, D.F. (1989) Meaning of coefficients and index of MCT soil classification for tropical soils. In *Proceedings of the 12th International Conference on Soil Mechanics and Foundation Engineering* (pp. 547-550). Rotterdam, Netherlands.

Nogami, J.S., & Villibor, D.F. (1991). Use of lateritic fine-grained soils in road pavement base courses. *Geotechnical* *and Geological Engineering*, 9(3-4), 167-182. http://doi.org/10.1007/BF00881739.

Pascoal, P.T. (2024). *Deformabilidade de subleitos de trechos monitorados da BR 116/RS considerando variações de umidade em laboratório e campo* [Doctoral thesis]. Universidade Federal de Santa Maria.

Pascoal, P.T., Sagrilo, A.V., Baroni, M., Specht, L.P., & Pereira, D.S. (2023). Lateritic soil deformability regarding the variation of compaction energy in the construction of pavement subgrade. *Soils and Rocks*, 46(3), e2023009922. http://doi.org/10.28927/SR.2023.009922.

Pezo, R.F., Carlos, G., Hudson, W.R., & Stokoe 2nd, K.H. (1992). *Development of reliable resilient modulus test for subgrade and non-granular subbase materials for use in routine pavement design.* Transportation Research Board. Retrieved in July 18, 2025, from https://trid.trb.org/view/369153.

Sagrilo, A.V., Pascoal, P.T., Baroni, M., Back, A.H., Pinheiro, R.J.B., Specht, L.P., & Guimarães, A.C.R. (2023). Contribution to resilient and permanent deformation investigation of unbound granular materials with different geological origins from Rio Grande do Sul, Brazil. *Soils and Rocks*, 46(3), e2023009822. http://doi.org/10.28927/SR.2023.009822.

Silva, M.F., Ribeiro, M.M.P., Furlan, A.P., & Fabbri, G.T.P. (2021). Effect of compaction water content and stress ratio on permanent deformation of a subgrade lateritic soil. *Transportation Geotechnics*, 26, 100443. http://doi.org/10.1016/j.trgeo.2020.100443.

Svenson, M. (1980). *Ensaios triaxiais dinâmicos de solos argilosos* [Master's dissertation]. Federal University of Rio de Janeiro repository.

Tseng, K.H., & Lytton, R.L. (1989). Prediction of permanent deformation in flexible pavement materials. In *Implication of aggregates in the design, construction, and performance of flexible pavements* (pp. 154–172). ASTM International.

Tutumluer, E., & Pan, T. (2008). Aggregate morphology affecting strength and permanent deformation behavior of unbound aggregate materials. *Journal of Materials in Civil Engineering*, 20(9), 617-627. http://doi.org/10.1061/(ASCE)0899-1561(2008)20:9(617).

Werkmeister, S., Dawson, A.R., & Wellner, F. (2001). Permanent deformation behavior of granular materials and the shakedown concept. *Transportation Research Record: Journal of the Transportation Research Board*, 1757(1), 75-81. http://doi.org/10.3141/1757-09.

Yoder, E.J., & Witczak, M.W. (1975). *Principles of pavement design*. New York: John Wiley & Sons Inc.. http://doi.org/10.1002/9780470172919.